



**HAL**  
open science

## Sonic disruption of wood pulp fibres aided by hydrophobic cavitation nuclei

Nicole Anderton, Craig Stuart Carlson, Albert Thijs Poortinga, Hu Xinyue, Nobuki Kudo, Michiel Postema

► **To cite this version:**

Nicole Anderton, Craig Stuart Carlson, Albert Thijs Poortinga, Hu Xinyue, Nobuki Kudo, et al.. Sonic disruption of wood pulp fibres aided by hydrophobic cavitation nuclei. *Japanese Journal of Applied Physics*, 2023, 62 (1), pp.018001. 10.35848/1347-4065/acaadd . hal-03895903

**HAL Id: hal-03895903**

**<https://hal.science/hal-03895903>**

Submitted on 13 Dec 2022

**HAL** is a multi-disciplinary open access archive for the deposit and dissemination of scientific research documents, whether they are published or not. The documents may come from teaching and research institutions in France or abroad, or from public or private research centers.

L'archive ouverte pluridisciplinaire **HAL**, est destinée au dépôt et à la diffusion de documents scientifiques de niveau recherche, publiés ou non, émanant des établissements d'enseignement et de recherche français ou étrangers, des laboratoires publics ou privés.



Distributed under a Creative Commons Attribution - NonCommercial - NoDerivatives 4.0 International License

ACCEPTED MANUSCRIPT

## Sonic disruption of wood pulp fibres aided by hydrophobic cavitation nuclei

To cite this article before publication: Nicole Anderton *et al* 2022 *Jpn. J. Appl. Phys.* in press <https://doi.org/10.35848/1347-4065/acaadd>

### Manuscript version: Accepted Manuscript

Accepted Manuscript is “the version of the article accepted for publication including all changes made as a result of the peer review process, and which may also include the addition to the article by IOP Publishing of a header, an article ID, a cover sheet and/or an ‘Accepted Manuscript’ watermark, but excluding any other editing, typesetting or other changes made by IOP Publishing and/or its licensors”

This Accepted Manuscript is © 2022 The Japan Society of Applied Physics.

During the embargo period (the 12 month period from the publication of the Version of Record of this article), the Accepted Manuscript is fully protected by copyright and cannot be reused or reposted elsewhere.

As the Version of Record of this article is going to be / has been published on a subscription basis, this Accepted Manuscript is available for reuse under a CC BY-NC-ND 3.0 licence after the 12 month embargo period.

After the embargo period, everyone is permitted to use copy and redistribute this article for non-commercial purposes only, provided that they adhere to all the terms of the licence <https://creativecommons.org/licenses/by-nc-nd/3.0>

Although reasonable endeavours have been taken to obtain all necessary permissions from third parties to include their copyrighted content within this article, their full citation and copyright line may not be present in this Accepted Manuscript version. Before using any content from this article, please refer to the Version of Record on IOPscience once published for full citation and copyright details, as permissions will likely be required. All third party content is fully copyright protected, unless specifically stated otherwise in the figure caption in the Version of Record.

View the [article online](#) for updates and enhancements.

## Sonic disruption of wood pulp fibres aided by hydrophobic cavitation nuclei

Nicole Anderton<sup>1</sup>, Craig S. Carlson<sup>1,2\*</sup>, Albert T. Poortinga<sup>3</sup>, Hu Xinyue<sup>4</sup>, Nobuki Kudo<sup>4</sup>, and Michiel Postema<sup>1,2</sup>

<sup>1</sup>*BioMediTech, Faculty of Medicine and Health Technology, Tampere University, Korkeakoulunkatu 3, 33720 Tampere, Finland*

<sup>2</sup>*School of Electrical and Information Engineering, University of the Witwatersrand, Johannesburg, 1 Jan Smuts Laan, 2001 Braamfontein, South Africa*

<sup>3</sup>*Department of Mechanical Engineering, Eindhoven University of Technology, De Zaaie, 5600 MB Eindhoven, The Netherlands*

<sup>4</sup>*Faculty of Information Science and Technology, Hokkaido University, Kita 14 Jo, Nishi 9 Chome, Kita-ku, Sapporo, Hokkaido 060-0814, Japan*

---

For paper manufacturing and biofuel production, the controlled deformation of wood pulp is of interest, provided that the integrity of the fibre structure remains intact. Conventional ultrasonic pretreatment in the near-audible range has been observed to cause uncontrolled inertial cavitation damage in the wood pulp fibres. To prevent internal damage, we proposed to subject wood pulp mixed with hydrophobic particles to 1-MHz short pulses above the nucleation threshold of the particles but below the Blake threshold, and to observe the interaction of pulsating cavities and wood pulp fibres assisted by high-speed photography. Our 1-MHz results showed the interaction of a collapsing bubble with a wood pulp fibre wall to form a liquid jet hitting the fibre, without apparent destruction of the structure, whilst our 20-kHz controls confirmed previously observed structural destruction. This study shows the feasibility of controlled wood fibre deformation at a high ultrasound frequency.

---

Wood pulp is used for making paper, but also of interest in the production of biofuel.<sup>1,2)</sup> The controlled deformation of wood pulp fibres is desired in processes where the cells need to be accessed by chemical agents and enzymes.<sup>1)</sup> In numerous independent studies, inertial cavitation generated during ultrasonic pretreatment of wood pulp fibres has been shown to not only increase the permeability of the cell walls, but also to disintegrate the structure of the fibres.<sup>3-6)</sup> Cavitation-induced permeation was recently confirmed in solid wood, as well.<sup>7)</sup> Whilst permeation is desirable in industrial processes, structural disintegration is not.<sup>1)</sup> As for the experimental settings in these prior studies, the inertial cavitation-generating ultrasonic

---

\*E-mail: craig.carlson@tuni.fi

apparatus used were operating in the near-audible frequency range, whilst sonication was varied from minutes to hours.<sup>3-6)</sup> Such acoustic conditions have been associated with the unwanted production of free radicals and deposition of heat.<sup>8-11)</sup> Pretreatment with steam has also been shown to lead to disruptive effects, such as the visible destruction of so-called boarded pits.<sup>12)</sup>

Under less powerful, clinical diagnostic sonication conditions, movement and permeation of cultured human and animal cells have been observed, too, but with less unwanted bioeffects.<sup>13-17)</sup> This type of ultrasound-assisted cell permeation requires the presence of microbubbles or cavitation nuclei in or near the cells under sonication.<sup>18-20)</sup> The asymmetric collapse of a pulsating microbubble near an interface has been observed to cause liquid jets impacting and penetrating the interface.<sup>21)</sup> As the interaction between cavitation nuclei and cells may happen within an ultrasound cycle, experimental optical observations are typically done aided by high-speed photography through a microscope system.<sup>22-24)</sup> We hypothesised that such a procedure would aid in the observation of wood pulp cell permeation, provided that the nucleation location is controlled to be outside the fibre rather than inside.

The purpose of this study was to subject wood pulp mixed with hydrophobic particles to ultrasound pulses of high enough acoustic amplitudes to cause the particles to nucleate but of low enough acoustic amplitude to prevent spontaneous inertial cavitation in different parts of the mixture.

At acoustic amplitudes high enough to generate inertial cavitation, microbubble-based nuclei are typically very short-lived, due to fragmentation processes.<sup>25,26)</sup> As an alternative to these rapidly destroyed nuclei, zinc oxide hydrophobic particles have been proposed for longer lasting nucleation.<sup>27)</sup> It has been observed, that the nucleation threshold of hydrophobic particles, but also of hydrophilic particles, is lower than the so-called Blake cavitation threshold.<sup>28-30)</sup>

Let us assume a perfectly spherical hydrophobic core comprising one or multiple particles surrounded by a bubble of a size proportional to this hydrophobic core and in suspension in an infinite liquid. Following the derivation steps previously presented,<sup>28)</sup> but including an additional damping term,<sup>31)</sup> the fundamental equation of radial hydrophobic particle dynamics can be stated as

$$R\ddot{R} + \frac{3}{2}\dot{R}^2 = \frac{1}{\rho} \left[ \left( p_0 - p_v + \frac{2\sigma R_0}{R_0^2 - R_h^2} \right) \left( \frac{R_0^3 - R_h^3}{R^3 - R_h^3} \right)^\gamma + p_v - \frac{2\sigma R}{R^2 - R_h^2} - \frac{4\eta\dot{R}}{R} - \delta\omega\rho R\dot{R} - p_0 - p(t) \right], \quad (1)$$

where  $p(t)$  is the time-dependent acoustic driving function,  $p_0 = 101$  kPa is the ambient pressure,  $p_v = 2.33$  kPa is the vapour pressure,  $R$  is the instantaneous bubble radius,  $R_0$  is the initial bubble radius,  $R_h \approx 0.1R_0$  is the incompressible hydrophobic core radius,  $\gamma = 1.4$  is the ratio of specific heats,  $\delta$  is the nonviscous part of the damping coefficient,<sup>31)</sup>  $\eta$  is the liquid viscosity,  $\rho = 998$  kg m<sup>-3</sup> is the liquid density,  $\sigma = 0.072$  N m<sup>-1</sup> is the surface tension, and  $\omega = 2\pi \times 10^6$  rad s<sup>-1</sup> is the angular driving frequency. We used a hydrophone recording of a single pulse of five ultrasonic cycles and peak-negative pressure amplitude 1.3 MPa as a driving function. This pulse had been recorded in a separate water container, with a hydrophone positioned along the central axis of the transducer and the hydrophone tip in the acoustic focus. The peak-negative pressure of the pulse was measured to be 1.3 MPa, whilst the peak-positive pressure was measured to surpass 7.4 MPa. As the inertial cavitation threshold is related to the rarefaction of a nucleus, only the peak-negative pressure was taken into account throughout the remainder of this study. It must be noted that (1) only applies until the moment that bubbles undergo surface harmonics or other asymmetries.

Bubble collapse close to an interface may result in a liquid jet protruding from the distal part towards and through the interface.<sup>32)</sup> The asymmetric collapse causes the part of the bubble distal to the interface to exceed the velocity of the proximal part to the interface. To conserve the impulse of the system, the liquid distal to the bubble is accelerated and focussed during collapse, leading to the formation of a liquid jet directed to and protruding through the interface.<sup>32)</sup> The protrusion may have a destructive effect on biomaterials.<sup>21)</sup> The radius of liquid jets has been empirically observed to relate to the collapsing bubble radius:<sup>33)</sup>

$$\frac{R_j}{R_c} \approx 0.1, \quad (2)$$

where  $R_c$  is the spherically symmetric pulsating bubble radius on the verge of collapse and  $R_j$  is the radius of the liquid jet. In addition, the length of the jet can be estimated from the following empirical relation:<sup>34)</sup>

$$\frac{l_j}{R_c} \approx 3, \quad (3)$$

where  $l_j$  is the full travel path of the liquid jet. It should be noted that the full liquid jet is rarely visible, because only the beginning of the protrusion, where gaseous components are drawn into the jet, has an optical refraction index different from the surrounding liquid medium.

Never dried unbleached softwood kraft pulp from a Scandinavian paper mill with a  $\kappa$  number of 85 was washed until a neutral pH was reached. The pulp was stored at 7 °C.

Prior to experiments, polypropylene conical tubes of 15-ml inner volume were filled with

5 ml of reverse-osmosis ultrapure (Type 1) water. To half of the tubes, 5 mg of Zano 10 Plus zinc oxide coated with octyl triethoxy silane (Umicore, Brussel, Belgium) was added. These hydrophobic particles had specified diameters of 50 nm. Although individual particles were too small for visual observation, microbubbles containing clusters of zinc oxide particles were visible. In each tube, 100 mg of wood pulp was deposited, after which the mixture was gently stirred for 1 minute.

An amount of 0.2 ml wood pulp mixture was pipetted into the observation chamber of a high-speed observation system,<sup>23)</sup> shown in Fig. 1a. The observation chamber was placed on top of an Eclipse Ti inverted microscope (Nikon Corporation, Minato-ku, Tokyo, Japan) with a Plan Apo 10×/0.45 WD 4.0 objective lens. An HPV-X2 high-speed camera (Shimadzu, Nakagyo-ku, Kyoto, Japan) was connected to the microscope. This camera was operating at a frame rate of ten million frames per second. The exposure time was 50 ns per frame. During camera recording, the material was subjected to one ultrasound pulse.

A laboratory-assembled single-element transducer produced focussed ultrasound pulses.<sup>23)</sup> Each pulse had a centre frequency of 1.0 MHz. The voltage amplitude of a pulse was 5.0 V. The signal fed into the transducer was generated by an AFG320 arbitrary function generator (Sony-Tektronix, Shinagawa-ku, Tokyo, Japan) and amplified by a UOD-WB-1000 wide-band power amplifier (TOKIN Corporation, Shiroishi, Miyagi, Japan). The pulse used as a driving function in the simulations had been created with these devices.

A total number of thirteen high-speed video sequences was recorded. Each video sequence consisted of 256 frames. These frames were imported into the matrix laboratory MATLAB<sup>®</sup> (The Mathworks, Inc., Natick, MA, USA). Nuclei sizes were measured and plotted as a function of time. The modified Rayleigh-Plesset equation (1) was numerically evaluated using the ode45 differential equation solver of MATLAB<sup>®</sup> for various liquid viscosities  $\eta \in \langle 10^0, 10^2 \rangle$  mPa s. The liquid viscosities used in the simulations included those stated in TAPPI standard 230 om-99. The simulated nucleation curves were superimposed on the measured nucleation plots.

In addition to high-speed photography experiments at 1-MHz sonication, near-audible controls were performed under literature settings, with and without zinc oxide present near wood pulp fibres. These control experiments served to rule out that any deviation with respect to experiments described in literature might be caused by the specific wood pulp sample or by the presence of zinc oxide.

For each near-audible control experiment, a conical tube was clamped such that its base was 12 mm below an FB4417 2-mm microtip (Thermo Fisher Scientific, Waltham, MA, USA)

with measured 1.6-mm diameter that was attached to a CL-334 ultrasound converter (Thermo Fisher Scientific) of an FB705 Sonic Dismembrator (Thermo Fisher Scientific), as shown in Fig. 1b. Each sample was sonicated at a frequency of 20 kHz for 5 min at an operating power of 700 W. The acoustic amplitude of this geometry corresponded to a mechanical index conservatively estimated to be at least twenty times the cavitation threshold. The temperature before and after sonication was measured using a mercury thermometer.

From each sonicated wood pulp mixture, two samples were extracted using tweezers, placed on microscope slides, and preserved with coverslips. Five regions of interest on each slide were optically evaluated using a Leica DMIL LED inverted microscope (Leica Microsystems, Wetzlar, Germany) with an N PLAN 20 $\times$  (NA 0.40, WD 0.39 mm) objective lens (Leica).

Representative controls in the near-audible frequency range are shown in Fig. 2. The controls demonstrated that under literature conditions, wood pulp fibres were disrupted. Visible disruption was observed both in presence and absence of zinc oxide. Under both conditions, boarded pits had deformed to noncircular geometries. These controls confirmed that the wood pulp sample was behaving similar under high-amplitude low-frequency sonication as described prior in literature. In addition, the presence of zinc oxide was not observed to alter the disruption caused by the near-audible ultrasound.

High-speed footage showed subsequent pulsation cycles of hydrophobic particles. The bubbles surrounding the particles were observed to have expanded to radii beyond 10  $\mu\text{m}$ . Fig. 3a shows a representative example of the radial excursion of hydrophobic zinc oxide near a wood pulp fibre as a response to the pressure pulse shown in Fig. 3b. Numerical solutions of (1) for a bubble of initial radius 2.9  $\mu\text{m}$  with a 10% incompressible core are shown in the same frame. The simulated outward excursions during the first cycles matched those of the experimental data points closest when choosing a liquid viscosity of 45 mPa s. The influence of surface tension or core size on the radial excursions were found to be negligible. Thus, the pulsations of the hydrophobic nuclei in our experiments were dominated by the viscous properties of the wood pulp.

From the fourth pulsation cycle on, radially asymmetric bubble oscillations were observed with a maximum radius of 30  $\mu\text{m}$ . At time stamp 11.2  $\mu\text{s}$ , an asymmetry was observed in the collapsing bubble, which may be interpreted as a jet protruding towards the wood pulp fibre interface, shown in Fig. 3c. The jet radius was estimated to be 2  $\mu\text{m}$ . Following (2),  $R_c \approx 20 \mu\text{m}$ . According to (3),  $l_j \approx 60 \mu\text{m}$ , which is well within the fibre. This empirical jet length is an indicator that the wood pulp fibre must have been disrupted following presumed

jet impact. It was noted that the boarded pits visible in the image sequence remained visibly intact in this event and the other experiments at 1 MHz. After the impact of the presumed jet, material was observed to stream near where the jet may have impacted (not shown), indicating successful jet penetration.

In conclusion, our 1-MHz results showed a collapsing bubble near a wood pulp fibre form a liquid jet hitting the fibre, without destruction of the structure, whilst our 20-kHz controls confirmed previously observed structural destruction. This study shows the feasibility of controlled wood fibre deformation at a high ultrasound frequency. To our knowledge, this paper presents the first photographic observation of ultrasound-assisted jet formation near a wood pulp fibre.

### Acknowledgements

This work was supported by JSPS KAKENHI, Grant Numbers JP17H00864 and JP20H04542, by the National Research Foundation of South Africa, Grant Number 127102, and by the Academy of Finland, Grant Number 340026.

**References**

- 1) K. Nyholm, P. Ander, S. Bardage, and G. Daniel, *Nord. Pulp Paper Res. J.* **16**, 376 (2001).
- 2) L. Zhang, A. Larsson, A. Moldin, and U. Edlund, *Ind. Crops Prod.* **187**, 115432 (2022).
- 3) T. Aimin, Z. Hongwei, C. Gang, X. Guohui, and L. Wenzhi, *Ultrason. Sonochem.* **12** 467 (2005).
- 4) Y. Xu, Y. Yan, X. Yue, Z. Zhu, D. Zhang, and G. Hou, *TAPPI J.* **13**, 37 (2014).
- 5) S. Zhou, Y. Li, L. Huang, L. Chen, Y. Ni, and Q. Miao, *Cellulose* **26**, 9287 (2019).
- 6) J. Qian, F. Zhao, J. Gao, L. J. Qu, Z. He, and S. Yi, *Ultrason. Sonochem.* **77**, 105672 (2021).
- 7) T. Tuziuti and K. Yasui, *Ultrason. Sonochem.* **88**, 106084 (2022).
- 8) J. Sostaric and L. K. Weavers, *Ultrason. Sonochem.* **17**, 1021 (2010).
- 9) T. Aikawa and N. Kudo, *Jpn. J. Appl. Phys.* **51**, SDDD13 (2021).
- 10) T. Moriyama, S. Yoshizawa, and S. Umemura, *Jpn. J. Appl. Phys.* **51**, 07GF27 (2012).
- 11) N. Obara, S. Umemura, and S. Yoshizawa, *Jpn. J. Appl. Phys.* **60**, SDDE04 (2021).
- 12) H. Dashi, A. Tarmian, M. Faezipour, S. Hedjazi, and M. Shahverdi, *BioResources* **7**, 1907 (2012).
- 13) L. B. Feril Jr., T. Kondo, Y. Tabuchi, R. Ogawa, Q.-L. Zhao, T. Nozaki, T. Yoshida, N. Kudo, and K. Tachibana, *Jpn. J. Appl. Phys.* **46**, 4435 (2007).
- 14) Y. Yamakoshi, T. Miwa, N. Yoshizawa, H. Inoguchi, and D. Zhang, *Jpn. J. Appl. Phys.* **49**, 07HF17 (2010).
- 15) R. Oitate, A. Shimomura, H. Wada, T. Mochizuki, K. Masuda, Y. Oda, R. Suzuki, and K. Murayama, *Jpn. J. Appl. Phys.* **56**, 07JF25 (2017).
- 16) R. Oitate, T. Otsuka, M. Seki, A. Furutani, T. Mochizuki, K. Masuda, R. Suzuki, and K. Murayama, *Jpn. J. Appl. Phys.* **57**, 07LF16 (2018).
- 17) D. M. Rubin, N. Anderton, C. Smalberger, J. Polliack, M. Nathan, and M. Postema, *Fluids* **3**, 82 (2018).
- 18) K. Tachibana and S. Tachibana, *Jpn. J. Appl. Phys.* **38**, 3014 (1999).
- 19) H. Yoshikawa, T. Azuma, K. Sasaki, K. Kawabata, and S. Umemura, *Jpn. J. Appl. Phys.* **45**, 4754 (2006).
- 20) B. Krasovitski, V. Frenkel, S. Shoham, and E. Kimmel, *Proc. Natl Acad. Sci.* **108**, 3258 (2011).
- 21) P. Prentice, A. Cuschieri, K. Dholakia, M. Prausnitz, and P. C. Campbell, *Nat. Phys.* **1**, 107 (2005).

- 1  
2  
3  
4  
5  
6  
7  
8  
9  
10  
11  
12  
13  
14  
15  
16  
17  
18  
19  
20  
21  
22  
23  
24  
25  
26  
27  
28  
29  
30  
31  
32  
33  
34  
35  
36  
37  
38  
39  
40  
41  
42  
43  
44  
45  
46  
47  
48  
49  
50  
51  
52  
53  
54  
55  
56  
57  
58  
59  
60
- 22) K. Suzuki, R. Iwasaki, R. Takagi, S. Yoshizawa, and S. Umemura, *Jpn. J. Appl. Phys.* **56**, 07JF27 (2017).
- 23) N. Kudo, *IEEE Trans. Ultrason. Ferroelect. Freq. Control* **64**, 273 (2017).
- 24) N. Okada, M. Shiiba, S. Yamauchi, T. Sato, and S. Takeuchi, *Jpn. J. Appl. Phys.* **57**, 07LE15 (2018).
- 25) J. E. Chomas, P. Dayton, D. May, and K. Ferrara, *J. Biomed. Opt.* **6** 141 (2001).
- 26) N. Kudo et al., *Jpn. J. Appl. Phys.* **59**, SKKE02 (2020).
- 27) M. Postema, R. Matsumoto, R. Shimizu, A. T. Poortinga, and N. Kudo, *Jpn. J. Appl. Phys.* **59**, SKKD07 (2020).
- 28) C. S. Carlson, R. Matsumoto, K. Fushino, M. Shinzato, N. Kudo, and M. Postema, *Jpn. J. Appl. Phys.* **60**, SDDA06 (2021).
- 29) S. I. Madanshetty and R. E. Apfel, *J. Acoust. Soc. Am.* **90**, 1508 (1991).
- 30) T. Tuziuti, K. Yasui, M. Sivakumar, Y. Iida and N. Miyoshi, *J. Phys. Chem. A* **109**, 4869 (2005).
- 31) N. Anderton, C. S. Carlson, V. Aharonson, and M. Postema, *Curr. Dir. Biomed. Eng.* **8**, 781 (2022).
- 32) A. Philipp and W. Lauterborn, *J. Fluid Mech.* **361**, 75 (1998).
- 33) T. Kodama and K. Takayama, *Ultrasound Med. Biol.* **24**, 723 (1998).
- 34) C. D. Ohl and E. Ory, *Phys. Rev. Lett.* **90**, 214502 (2003).

### List of Figures

**Fig. 1.** Experimental high-speed photography setup (a), comprising a 1-MHz single-element focussed ultrasound transducer (i), a water-filled container (ii), an observation chamber (iii), and an objective lens (iv); experimental setup for near-audible controls (b), comprising a microtip (v), a conical tube (vi), a clamp (vii), and a dismembrator (viii).

**Fig. 2.** Wood pulp fibres before near-audible sonication (a), after 5-min sonication (b); wood pulp fibres mixed with zinc oxide, whose clusters are indicated by dashed green circles, before sonication (c) and after 5-min sonication (d).

**Fig. 3.** Radial response (a) of a hydrophobic core subjected to a pressure pulse whose peak-negative pressure was 1.3 MPa (—) and whose peak-positive pressure surpassed 7.4 MPa (b), measured from high-speed video footage of hydrophobically modified zinc oxide (○) and simulated for a bubble of radius  $R_0 = 2.9 \mu\text{m}$  with a 10% incompressible core in a medium with 45-mPa s viscosity. Inlays extracted from high-speed video footage each correspond to a 100- $\mu\text{m}$  diameter. A zinc oxide cluster is highlighted by a dashed green circle. Selected high-speed footage (c) of an area corresponding to  $150 \times 150 \mu\text{m}^2$  with schematics overlain show a bubble at its maximum (i), its collapse to form a liquid jet (ii), and a composite image of both frames (iii).

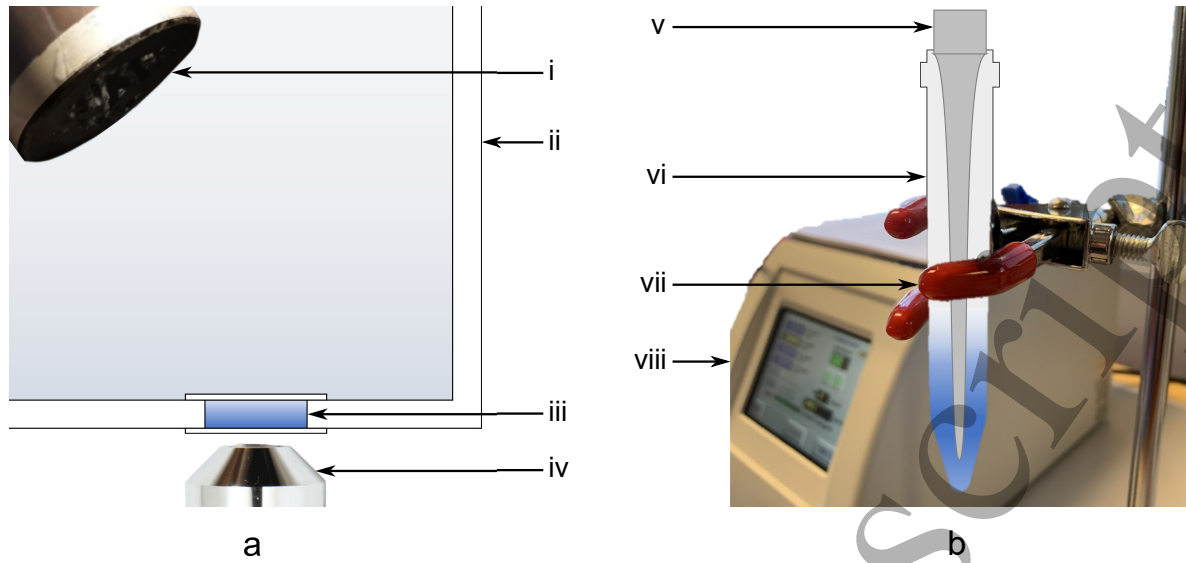


**Fig. 1.** Experimental high-speed photography setup (a), comprising a 1-MHz single-element focussed ultrasound transducer (i), a water-filled container (ii), an observation chamber (iii), and an objective lens (iv); experimental setup for near-audible controls (b), comprising a microtip (v), a conical tube (vi), a clamp (vii), and a dismembrator (viii).

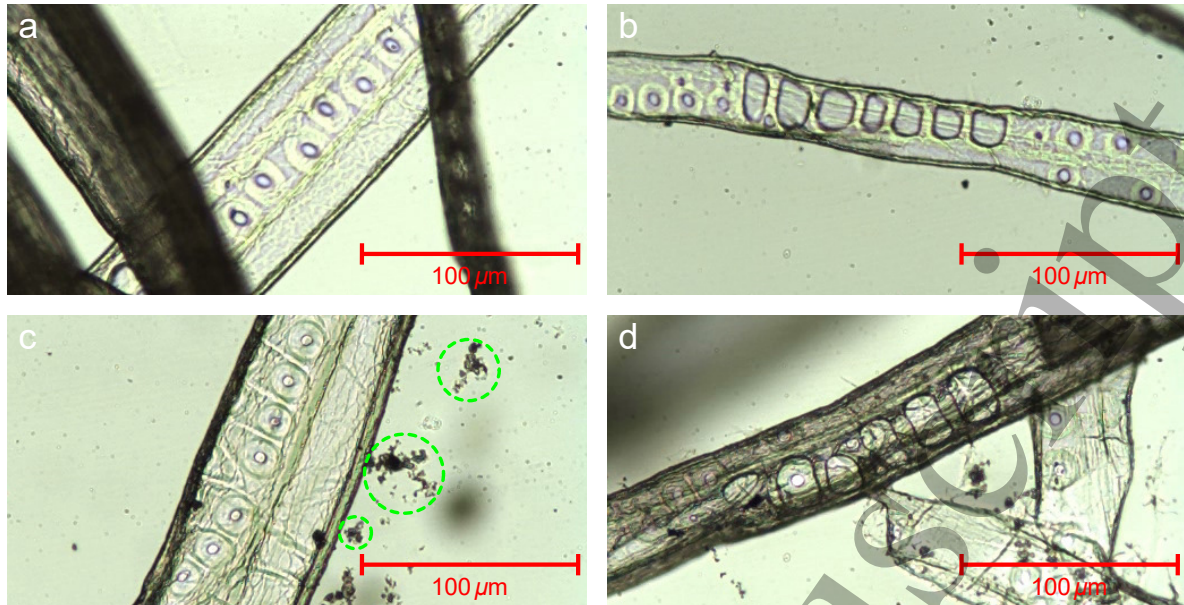


**Fig. 2.** Wood pulp fibres before near-audible sonication (a), after 5-min sonication (b); wood pulp fibres mixed with zinc oxide, whose clusters are indicated by dashed green circles, before sonication (c) and after 5-min sonication (d).

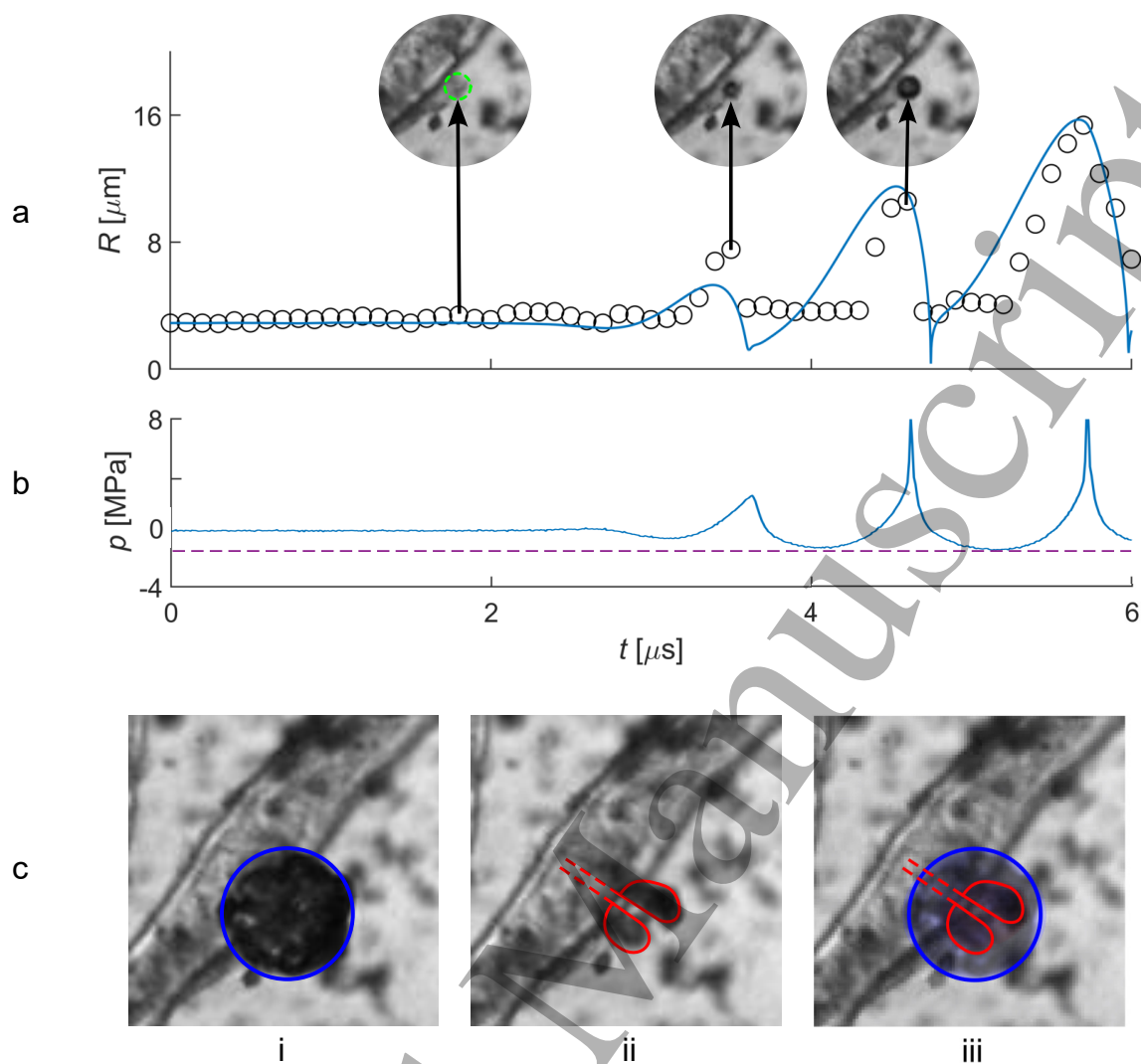


**Fig. 3.** Radial response (a) of a hydrophobic core subjected to a pressure pulse whose peak-negative pressure was 1.3 MPa (---) and whose peak-positive pressure surpassed 7.4 MPa (b), measured from high-speed video footage of hydrophobically modified zinc oxide ( $\circ$ ) and simulated for a bubble of radius  $R_0 = 2.9 \mu\text{m}$  with a 10% incompressible core in a medium with 45-mPa s viscosity. Inlays extracted from high-speed video footage each correspond to a 100- $\mu\text{m}$  diameter. A zinc oxide cluster is highlighted by a dashed green circle. Selected high-speed footage (c) of an area corresponding to  $150 \times 150 \mu\text{m}^2$  with schematics overlain show a bubble at its maximum (i), its collapse to form a liquid jet (ii), and a composite image of both frames (iii).